Journal of Cleaner Production 276 (2020) 123198

Contents lists available at ScienceDirect

Journal of Cleaner Production

journal homepage: www.elsevier.com/locate/jclepro

Simultaneous brewery wastewater treatment and hydrogen generation via hydrolysis using Mg waste scraps

R. Akbarzadeh [a, *], J.A. Adeniran [b], M. Lototskyy [c], A. Asadi [d]

[a] Energy, Sensors and Multifunctional Nanomaterials Research Group, Department of Chemical Sciences, Faculty of Science, University of Johannesburg, Doornfontein, 2028, South Africa
[b] Department of Mechanical Engineering Science, University of Johannesburg, Auckland Park Kingsway Campus, Johannesburg, 2006, South Africa
[c] HySA Systems Competence Centre, South African Institute for Advanced Materials Chemistry (SAIAMC), University of the Western Cape, Bellville, South Africa
[d] Research Center for Environmental Determinants of Health (RCEDH), Health Institute, Kermanshah University of Medical Sciences, Kermanshah, 67146, Iran

ARTICLE INFO

Article history:
Received 31 January 2020
Received in revised form
1 July 2020
Accepted 2 July 2020
Available online 24 July 2020

Handling editor: Dr Sandra Caeiro

Keywords:
Brewery wastewater
Treatment
Hydrogen generation
Hydrolysis
Mg scrap

ABSTRACT

An advanced, eco-efficient "waste plus waste to hydrogen" method was developed for hydrogen generation and the simultaneous treatment of two types of waste generated from magnesium and brewery-based industries via hydrolysis. The hydrolysis of Mg scraps was carried out using brewery wastewater and the reaction was accelerated with acetic acid (aa) at different concentrations (0, 12, 18, 24 and 30 wt% aa). The concentration of pollutants such as cyclortisiloxane-hexamethyle ($C_6H_{18}O_3Si_3$), which are persistent in conventional wastewater treatment, was successfully reduced. After the hydrolysis of the wastewater, 62.4% of chemical oxygen demand (COD) reduction and the complete colour removal were observed. The highest hydrogen generation, about 0.99 NL/min (>60% H_2 yield in 5 min), was observed in the presence of 30 wt% aa concentration in the hydrolysis reaction. This study proposes an eco-efficient hydrogen generation and waste treatment method as it simultaneously degrades pollutants and produces hydrogen utilizing Mg scrap waste and brewery wastewater without additional energy consumption.

1. Introduction

Water and energy are two of the most important issues of today's world. A lot of research has been done or is in progress to improve water and wastewater treatment technology. In addition, there have also been efforts to utilize waste as a source of energy which, at the same time reduces pollution. Most of the water from natural sources is polluted due to wastewater as a consequence of industry. Many different chemicals are discharged into the aquatic environment through industrial activities which pose a risk to human health and the environment. Some of them are persistent, toxic and partly biodegradable; hence, they are not easily removed in conventional wastewater treatment plants (Patwardhan, 2017; Akbarzadeh et al., 2016). Therefore there is a need to develop an eco-efficient method for the treatment of this kind of pollutant, which can treat the wastewater efficiently and economically.

The brewing industry is water intensive and consequently produces huge volumes of wastewater. The wastewater from these industries also leads to soil pollution in the cases of inappropriate treatment and land discharge (Pant and Adholeya, 2007). It is reported that it can inhibit seed germination, reduce soil alkalinity, cause soil manganese deficiency and damage agricultural crops (Kannabiran and Pragasam, 1993; Pandey and Agrawal, 1994). Various conventional and advanced methods have been introduced for the treatment of brewery wastewater (Simate et al., 2011; Werkneh et al., 2019). The conventional biological treatment includes anaerobic treatment with recovery of biogas, followed by aerobic treatment. However, some of the reported compounds in this type of wastewater like phenolic wastewater (Herrmann and Janke, 2001; Shah and Podriguez-Couto, 2019) are not readily biodegradable and therefore cannot be removed conventionally. Although several technologies have been suggested for brewery wastewater treatment which are efficient, implementing them such that they meet government environmental regulations is

* Corresponding author.
E-mail address: rakbarzadeh@uj.ac.za (R. Akbarzadeh).

https://doi.org/10.1016/j.jclepro.2020.123198
0959-6526/

costly and relatively complex (Simate et al., 2011; Kanagachandran and Jayarante, 2006). In addition, most of these available conventional bio-hydrogen production methods need pretreatment (Sharmila et al., 2020) which further complicates the process. Moreover, the cost of energy causes concerns in addition to the discharge of effluents to water bodies. The application of advanced alternative treatment methods is necessary to meet environmental legislation for wastewater discharge.

Apart from the importance of water, energy is another essential factor. Economic, social and physical activities rely on the supply of energy. Fossil fuels such as oil which are in use for supply of energy are depleting, and in addition these sources of energy are not clean. Although H_2 can be produced using many techniques (Ni et al., 2006), its production requires other sources. Therefore, finding a sustainable alternative source of energy is necessary. These days, hydrogen is considered a clean energy carrier that can be produced by different methods and from different sources including fossil fuels. Therefore, significant effort has been put into find the cost-effective hydrogen production method (Celik and Yildiz, 2017).

Magnesium can produce hydrogen through hydrolysis when it comes into contact with water (Uan et al., 2009). However, the by-product of hydrolysis, $Mg(OH)_2$, can cover the surface of metal and then decrease the hydrogen generation yield. Considerable research has been conducted to improve the yield of hydrogen production by hydrolysis. Application of acids such as acetic acid, citric acid, nitric acid and salts such as sodium chloride, can accelerate the hydrolysis kinetic and hydrogen generation process (Uan et al., 2009; Kushch et al., 2011).

Brewery wastewater contains chemical reagents such as weak acids (Mielcarek et al., 2013) which can also act as a conditioning agent to enhance the yield of hydrogen production; in addition it is a source of water for hydrolysis. Producing hydrogen from brewery wastewater has been proposed and practiced by many researchers using different methods such as dark fermentation and microbial fuel cell (Sharmila et al., 2020; Simate et al., 2011; Maintinguer et al., 2017; Engida et al., 2020; Das and Mangwani, 2010). However, these methods are not cost-effective because they need additional sources of energy. Additionally, these processes present challenges as the wastewater contains toxic organic compounds such as phenolic compounds which can be mutagenic, carcinogenic, and are environmental endocrine disrupters (Ni et al., 2006; Mohanakrishna et al., 2010; Chandra and Kumar, 2017).

Moreover, recently, recycling of magnesium, especially end-of-life Mg products has become increasingly important because of the increasing use of the metals in consumer electronics and in transportation, since it is so lightweight, and thus improves fuel economy (Uan et al., 2007). However, at present, recycling of all low-grade Mg scrap is not economically possible. On the other hand, as mentioned above, hydrolysis of Mg is a facile and cost-effective hydrogen production method. Low-grade magnesium, which is solid waste originating from industries that use metals such as electronics and transportation, cannot be recycled economically because of constraints in the refining technology (Friedrich and Mordike, 2006; Bell et al., 2006). During the last decade, however, H_2 generation by hydrolysis of Mg-based materials such as Mg and MgH_2 in pure water or at the presence of other chemicals has been studied extensively (Grosjean and Roué, 2006).

Metals are considered as expensive non-renewable resources which produce metal waste including magnesium. Recycling is a cost effective and environmentally friendly method for the usage of metals waste. However, because of the lack of proper refining and recycling industries, recycling of low-grade Mg scraps is not possible, and most of it is burnt or buried (Matković et al., 2014). Recently, the production of hydrogen using Mg scraps has attracted researchers' attention, presenting an alternative to manage Mg-based waste economically. Mg scrap is a potential source for economical hydrogen generation.

Hydrogen is likely to become a main source of fuel in the near future and to secure a sustainable H_2 production and supply, a renewable source for the production of H_2 must be developed. This is where the role of Mg waste for the production of high-purity hydrogen can be utilized in concert with other industrial waste such as brewery wastewater as a source of water. In addition, the by-product of hydrolysis of Mg can be recycled and used for different applications (Uesugi et al., 2010).

In this study, we have developed a novel waste plus waste chemical hydrogen generation method for simultaneous waste treatment and hydrogen production while utilizing two type of waste from two different industries as the raw materials. The Mg scrap was exposed to wastewater for the hydrogen generation while partial treatment of wastewater occurred. The acetic acid (*aa*) was used to enhance the hydrolysis kinetic. This advanced waste plus waste treatment technology provides an innovative and eco-efficient solution to three major industrial issues; Mg solid waste mitigation, brewery wastewater treatment and hydrogen production. Other studies have examined hydrogen generation from hydrolysis of Mg and Mg-based scraps in citric acid-added seawater or in aqueous solutions of NaCl (Uan et al., 2007, 2009). However, the novelty of this study is additional reduction of organic pollutant in brewery wastewater via a hydrolysis technique while producing hydrogen. To the best of our knowledge, simultaneous pollutant degradation and hydrogen production by hydrolysis using Mg waste scraps has not been reported elsewhere.

2. Material and methods

2.1. Material

Mg scrap waved plates coupled with stainless-steel mesh (Fig. 1) were received from National Chung Hsing University, Taiwan. This material was prepared and used by Uan and his colleagues for hydrolysis to generate hydrogen from seawater with the additive of citric acid (Uan et al., 2009). These plates were cut into smaller pieces (weight of 3.8 g) used for hydrogen generation in hydrolysis reaction experiment. Fig. 1 represents the photograph of Mg scrap waved plates used for hydrogen generation in this study.

Acetic acid (60.05%) was purchased from Labchem, South Africa and used with no further treatment. Wastewater samples were collected from a local brewery in Johannesburg. The EC (Electroconductivity) and COD (Chemical Oxygen Demand) of the actual brewery wastewater sample at pH 6.17 and temperature of 22.7 °C were measured to be 3.09 S/m and 6130 mg/l, respectively.

2.2. Hydrogen production setup

Hydrolysis was used as the method for hydrogen production. The hydrogen production set up reported earlier was used by Adeniran et al. (2019). At the start of each experiment, the sample of Mg scrap (3.8 g net weight) was placed inside the reaction vessel. Brewery wastewater was used as a source of water and mixed with aa for hydrolysis. All experiments were conducted in a water bath set at 50 °C.

To study the effect of different experimental conditions, three different parameters, *aa* concentration, solution volume and presence of stainless steel mesh, were varied as is shown in Fig. S1; see Supplementary Material. The hydrolysis experiments were conducted with 50, 100 and 200 ml wastewater solution, respectively, to ascertain the impact of water/acid to substrate ratio on hydrogen yield. Various concentrations of aa in wastewater) were examined for hydrogen yield, namely: with aa concentrations of 12, 18, 24 and

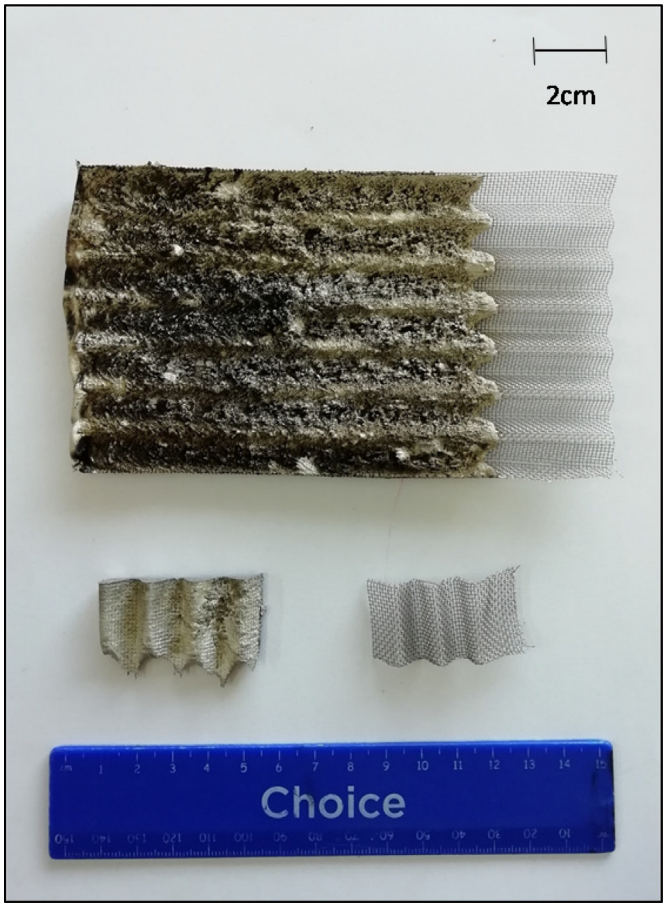

Fig. 1. Mg scrap waved plate coupled with stainless-steel mesh (top) and the cut Mg scrap plate (bottom left) and stainless-steel mesh (bottom right).

30 wt%. When studying the effect of stainless-steel mesh on hydrogen generation, the investigated samples included: (a) a 4.8 g piece of the as-delivered Mg scrap, or (b) a piece of the Mg scrap of the same gross weight after removal of the stainless steel mesh (1 g in the weight). In all the experiments, the net weight of the Mg-containing sample was 3.8 g.

More details about procedure of the hydrolysis experiments is presented in Supplementary Material, Fig. S2 and comment thereafter.

2.3. Characterization of Mg scrap

To study the phase composition of used material and the by-product, X-ray diffraction (XRD) characterization was carried out for Mg scrap before hydrolysis and Mg scrap residues after hydrolysis. A Bruker AXS D8 Advance instrument (USA) was used and the patterns with a Cu Kα ($\lambda = 1.5406$ Å) radiation were taken over the diffraction angle (2θ) range of 10–90°. Scanning electron microscopy (SEM) was carried out for the samples before and after hydrolysis using a Vega 3 Tecan scanning electron microscope operated at 20 kV accelerating voltage using a secondary electron detector. The elemental composition of the Mg scrap and its residual were ascertained using elemental energy dispersive x-ray spectroscopy (EDS) coupled with SEM.

2.4. Characterization of wastewater

The pH and electrical conductivity (EC) of the solution were measured at ambient temperature (22.7–22.9 °C) using a Hanna Instruments multifunction portable EC meter (USA). The chemical oxygen demand (COD) concentration in the wastewater before and after hydrolysis were measured using the closed reflux colorimetric method (DR3900). Fourier transform infrared spectroscopy (FTIR) of the samples was applied in the range of 400–4000 cm^{-1} by a diamond ATR fitted FTIR. The FTIR allows the characterization of a chemical structure by identifying the functional groups present in each sample. The GC-MS analysis of the samples (*aa* solution, wastewater, wastewater + *aa*) was done using a Shimadzu QP2010 Ultra mass spectrometer interfaced to a gas chromatograph in splitless injection mode. Scanning was done for 35 min with the scan rate of 2 scans per second and the component identification was achieved with Shimadzu post run software and NIST mass spectral library.

3. Results and discussion

3.1. Characterization of Mg- scrap before and after hydrolysis

Fig. 2 a1 shows SEM images of the Mg- scrap and the corresponding EDS spectrum is presented in Fig. 2 a2. As can be seen from Fig. 2 a2, the major component of the scrap is magnesium, with impurities of aluminium and silicon. Noticeable amounts of carbon (due to contribution of the sample holder) and oxygen (due to sample oxidation) are also clearly seen. The estimation of amounts of the components in the bulk sample (when taking into account carbon and oxygen) yielded 1.4 wt% Si, 10.1 wt% Al and 88.5 wt% Mg. The latter value corresponds to 3.36 g Mg in the sample taken for the hydrolysis (m = 3.8 g without stainless steel mesh).

Rietveld refinement of XRD pattern of the as-received Mg scrap (see Fig. 3) showed that the major phase (>90 wt %) has Mg structure (space group $P6_3/mmc$, #194) but with lower lattice periods and unit cell volumes than the values reported for pure Mg ($a = 3.2095$ Å, $c = 5.2107$ Å, $V = 46.4858$ $Å^3$ (Von Batchelder and Raeuchle, 1957). It is caused by the substitution of Mg (atomic radius R = 1.50 Å) with the smaller atoms of Al (R = 1.25 Å) in the Mg–Al solid solution phase. Furthermore, the quality of the refinement significantly improved when assuming the presence of several Mg–Al phases with close but different lattice periods. Fig. 3 illustrates this feature assuming presence of two phases: Mg–Al (1) (43.8 wt%; $a = 3.19336(6)$ Å, $c = 5.1897(2)$ Å, $V = 45.832(2)$ $Å^3$) and Mg–Al (2) (46.5(1) wt.%; $a = 3.17686(7)$ Å, $c = 5.1676(2)$ Å, $V = 45.166(2)$ $Å^3$). Comparison of the observed values of the unit cell volumes with literature data (Von Batchelder and Raeuchle, 1957; Hardie and Parkins, 1959; Saccone et al., 2002), which shows a linear dependence of the unit cell volume for Mg–Al solid solutions on the content of Al (0–10 at. %), allowed us to calculate Al concentrations in the Mg-rich phases in the sample to be 4.1 and 8.3 at.% Al, for the phases Mg–Al (1) and Mg–Al (2), respectively. The studied sample also contained 9.7(1) wt.% of γ-$Mg_{17}Al_{12}$ (space group $I\bar{4}3m$, #217) with calculated lattice period, $a = 10.5791(4)$ Å, close to the value reported in the literature (Saccone et al., 2002).

Quantitative estimations on the basis of the XRD results show that the overall content of Al in the studied sample was about 12.2 wt%, and the weight of Mg in 3.8 g sample taken for the hydrolysis was of 3.34 g which corresponds well to the EDS results.

As can be seen from Fig. 4, the interaction of compact pieces of Mg scrap with solutions of aa in brewery wastewater results in disintegration of the samples and their dissolution which generally increases with the increase of the *aa* concentration. The residual of Mg scrap (starting weight 3.8 g for the each hydrolysis experiment) after its hydrolysis with 100 ml of wastewater solution containing 30, 24, 18 and 12% aa had weight of 0.18 (b; 4.7% of the starting weight), 0.58 (c;

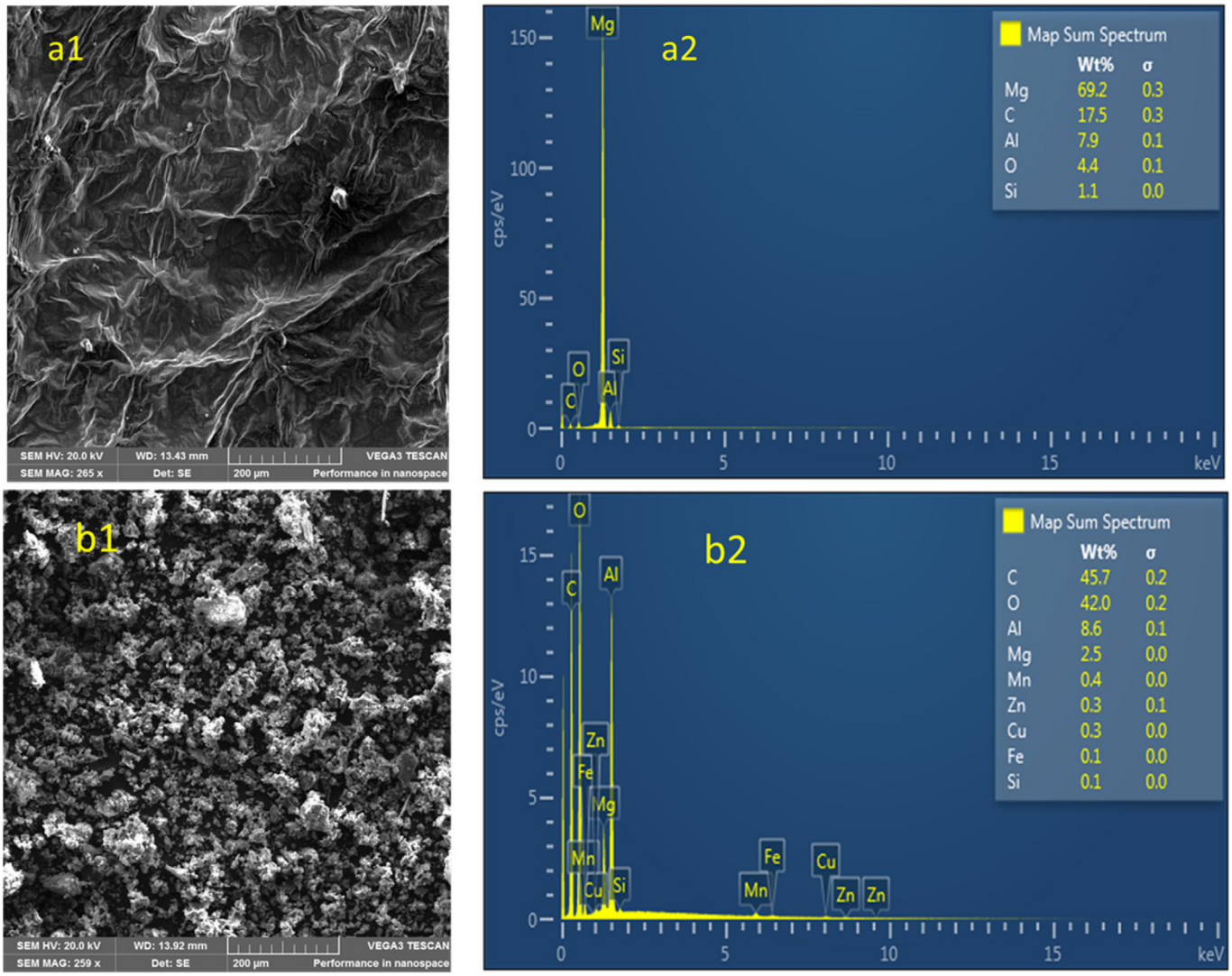

Fig. 2. SEM micrographs of (a1) Mg scrap before hydrolysis, (b1) Mg scrap residual after hydrolysis with wastewater containing 24% aa (the length of scale bars are equal to 200 µm), (a2) EDS spectrum of a1, and (b2) EDS spectrum of b1.

15.3%), 2.5 (d; 65.8%) and 1.2 g (e; 31.6%), respectively.

SEM images in Fig. 2, show that during hydrolysis the compact pieces of Mg scrap (a1) were disintegrated into fine particles (b1). Obviously, the defragmentation of initial pieces of the Mg scrap facilitates its contact with the hydrolysis solution by creating new solid − liquid interfaces and thus promoting further hydrolysis. It also can be seen from Fig. 2 (compare a2 and b2) that hydrolysis results in the drop of Mg concentration in the solid residue along with significant increase of the concentration of carbon, oxygen and aluminium, as well as the appearance of trace amounts of other elements (Mn, Zn, Cu, Fe) not detected in the sample before the hydrolysis.

The observations described above allow us to conclude that hydrolysis reactions under experimental conditions result mainly in the dissolution of Mg, according to Reactions 1 and 2 (see section 3.2 below). Accordingly, the deposit will contain insoluble compounds (hydroxides or acetate hydroxides) of Al or Al−Mg.

Indeed, the main phases identified on the XRD pattern of the residual after hydrolysis (see Fig. 5) were aluminium acetate hydroxide, $Al(OH)(CH_3COO)_2$ (Xavier et al., 1998); structure not reported) and $Al(OH)_3$ (bayerite; space group $P12_1/c1$, #14 (Rothbauer et al., 1967). The third phase, most probably, relates to mixed magnesium-aluminium acetate hydroxide hydrate, $(Mg,Al)(OH)(CH_3COO)_2{*}xH_2O$, with a structure similar to magnesium-aluminium carbonate hydroxyl hydrate (hydrotalcite; space group $P12_1/c1$, #14) (Radha et al., 2007). It was noted that hydrotalcite-like compounds, or anionic clays, are layered double hydroxides formed by a stacking of positively charged sheets (which contain Mg^{2+}, Al^{3+} and other cations, together with OH^- anions) separated by interlayer spaces containing solvated anions (CO_3^{2-}, Cl^-, organic anions) (Radha et al., 2007; Adachi-Pagano et al., 2003). Frequently, these compounds are formed as a result of hydrolysis (Adachi-Pagano et al., 2003). Similarly layered structures were shown to be formed by aluminium acetate hydroxide macromolecules (Sui et al., 2018).

3.2. Hydrogen generation via hydrolysis

The interaction of Mg with water can be described as:

$$Mg + 2H_2O \rightarrow Mg(OH)_2 + H_2 \quad (1)$$

According to Reaction 1, 1 g of Mg metal is able to generate 0.92 NL H_2, at the minimum (stoichiometric) amount of water of 1.48 g. Therefore, the theoretical H_2 generation for 3.8 g of Mg is 3.496 NL,

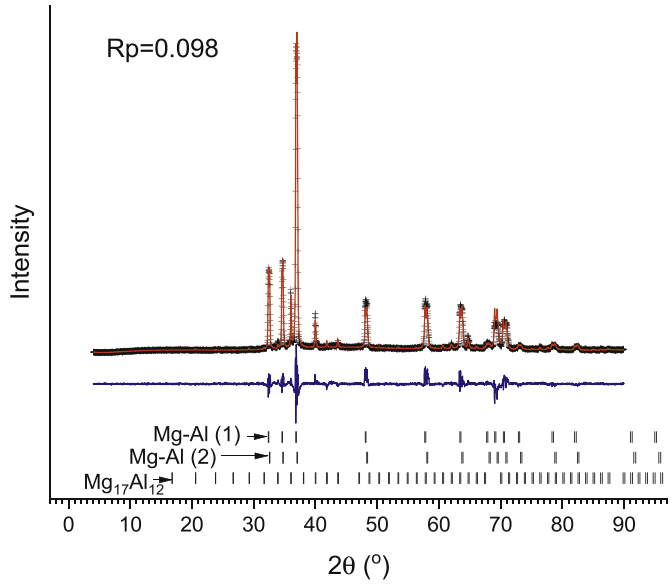

Fig. 3. Rietveld refinement of the XRD pattern of Mg scrap before hydrolysis. Points – observed, red line – calculated, blue bottom line – (observed–calculated). Bottom labels correspond to peak positions of the identified phases. (For interpretation of the references to colour in this figure legend, the reader is referred to the Web version of this article.)

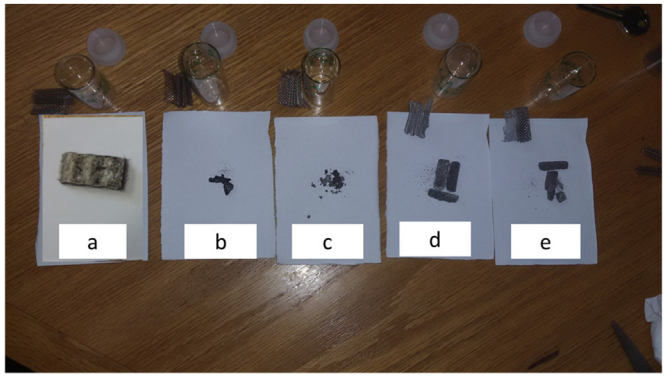

Fig. 4. Mg scrap before (a) and after (b–e) hydrolysis reaction with 100 ml solution of aa in brewery wastewater, with concentrations of 30% (b), 24% (c), 18% (d) and 12% (e). The residuals (b–e) were recovered after 1 h of the hydrolysis reaction.

however, as shown by EDS and XRD (Section 3.1), the weight percentage of Mg in the bulk scrap is 88.5% and consequently the theoretical H_2 value will be 3.10NL.

3.2.1. *Effect of aa on hydrogen evolution by hydrolysis of Mg scrap and brewery wastewater*

In this study aa was used to accelerate hydrolysis of Mg for hydrogen generation and to avoid the formation of a passivation layer. Reaction 2 represents the interaction of aa with magnesium hydroxide which forms the passivation layer:

$$Mg(OH)_2 + 2CH_3COOH \rightarrow Mg(CH_3COO)_2 + 2H_2O \quad (2)$$

In fact, presentation of hydrolysis of magnesium in aa solutions as Reactions 1 and 2 is a convenient simplification of the balance of real process which involves a large number of steps related to charge and mass transfer between aqueous solution, H_2 gas and their interfaces with several solid phases. Thus the overall reaction

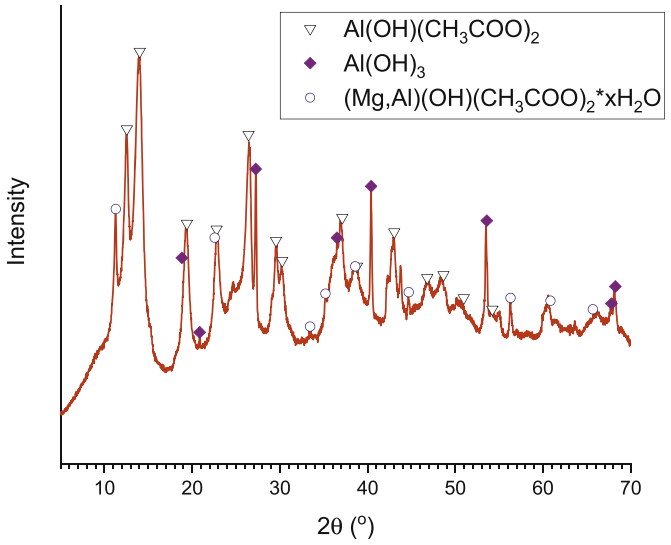

Fig. 5. XRD pattern of the residual after 1 h hydrolysis of Mg- scrap with 100 ml 24%aa.

kinetics will be very sensitive to the variations of external conditions (first of all, concentration of the acid in the solution) which may change the rate-determining step (Casey and Bergeron, 1953).

Fig. 6 shows hydrogen generation from 3.8 g of Mg scrap, with different concentrations of aa (12, 18, 24 and 30 %aa) added to wastewater with total solution volume of 100 ml. It could be observed that within the first 5 min the amount of produced hydrogen was equal to 0.7, 1, 1.5 and 2 NL for the *aa* concentration of 12, 18, 24 and 30 wt% respectively.

As discussed, aa improves the kinetics of the hydrolysis. The performance of hydrolysis in terms of hydrogen generation rate was as follows: 30 ≈ 24>18 > 12 wt% *aa*. Within the first 2 min, hydrolysis at the presence of 24–30% *aa* had the fastest kinetic of the hydrogen generation. Thus higher aa concentrations accelerate hydrogen evolution from the Mg scrap. Less pronounced kinetic improvements at *aa* concentrations above 24 wt% may have their origin in the inhibition of the process due to modification of its rate-limiting step in the concentrated solutions (Casey and Bergeron, 1953).

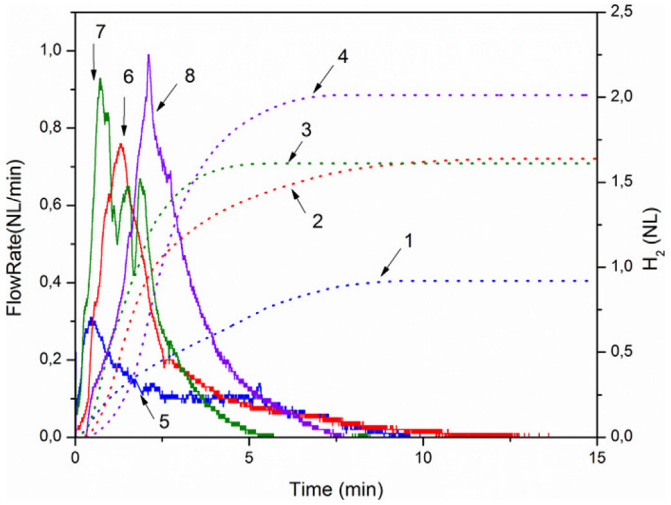

Fig. 6. Effect of aa concentration of on H_2 generation volume (1,2,3 & 4 for 12, 18, 24 and 30 wt% aa) and flowrate (5,6,7 & 8 for 12, 18, 24 and 30 wt% aa) using Mg scrap and brewery wastewater.

The effect of the solution volume (12 wt% *aa*) on hydrogen generation is illustrated by Fig. S3 in Supplementary Information. As can be seen, with the increase of solution volume at the same amount of Mg scrap, the flow rate and the volume of H_2 generation also increase. The amount of H_2 released during 15 min in the case of the 200 ml solution was about 0.88 NL compared to 0.67 NL for 100 ml solution and 0.65NL for 50 ml solution. Interestingly, it could be observed that the hydrogen yield achieved after 60 min for 200 ml wastewater with 12% *aa* concentration was 2 NL (Fig. S3, curve 3) and was approximately equal to the H_2 yield produced by 100 ml wastewater with 30% of *aa* (Fig. 6, curve 4). It clearly indicates that the increase of the wastewater volume could reduce the usage of *aa*. However, hydrogen release during the first 5 min in 100 ml wastewater with 30% of *aa* was faster than in 200 ml wastewater with 12% *aa*.

Fig. S3 also shows that the reaction begins spontaneously and after the first few minutes of *ww* contact with Mg scraps a steady evolution of hydrogen gas (H_2) takes place.

The effect of stainless steel mesh on H_2 generation was also studied using 200 ml of wastewater containing 12 wt% aa solution (see Fig. S4 in Supplementary Information). Initially the kinetic of the reaction was slightly faster in the presence of stainless steel mesh, however, after 15 min of hydrolysis, the hydrogen generation rate increased for the Mg scrap sample without metallic mesh (Fig. S4). Therefore, there was no significant difference between the H_2 generation using scrap with and without metallic mesh, as clearly shown in Fig. S4. The remaining hydrolysis experiments were carried out without stainless steel mesh.

The results of hydrogen generation via hydrolysis changing different variables have been summarized in Table S1 presented in the Supplementary Information.

Taking into account the amount of Mg used in each experiment (3.8*88.5/100 = 3.363 g) and stoichiometry of Reactions 1 and 2, their completion accompanied by the release of 3.10 NL H_2, as mentioned above, requires 4.99 g of H_2O (Reaction 1) and 16.62 g of CH_3COOH (Reaction 2). As can be seen from Table S1, different excesses/shortages of the aa as compared to the stoichiometry of Reaction 2 (from 63.9% shortage to 80.5% excess) were tried in the hydrolysis experiments. The variation was for the identification of the influence of the excess/shortage of the aa as compared to the stoichiometry of Reaction 2, since for all the cases the water was in a high excess (10x to 40x) as compared to stoichiometry of Reaction 1.

Fig. 7 shows dependence of the reaction yield after 15 min of the hydrolysis (a) and the maximum rate of H_2 evolution (b) on the shortage or excess of the aa in the reaction solution (Table S1). A clear correlation shown by dashed lines can be seen. The irregularities were mostly observed as negative deviations from the general trend and included: (i) lowering hydrogen yield in the concentrated solutions (Fig. 7a), as well as slowing the kinetics down (ii) at the lower *aa* concentrations and/or (iii) when the solution volume increased (Fig. 7b). These features can be explained by the changes of the reaction mechanisms including limitations of the solubility of the magnesium acetate formed during Reaction 2 (i), longer diffusion pathways in higher solution volume (iii) and the acceleration of the surface processes at higher *aa* concentrations (ii).

3.2.2. Effect of hydrolysis on wastewater treatment

To evaluate the efficiency of the method for simultaneous hydrogen production and wastewater treatment, the actual wastewater from a brewery industry was used and wastewater samples before addition of acid, after addition of acid and after hydrolysis reaction were characterized by COD, EC, and pH. The effect of hydrolysis on wastewater characteristics has been shown in Table 1. It could be seen that the COD of wastewater reduced by 62.4% which is a significant reduction while hydrogen was produced via hydrolysis. The EC of wastewater was increased due to the formation of magnesium acetate which is an ionic compound soluble in water thus increasing the electroconductivity of the solution. The pH of solution after adding *aa* quickly reduced to 1.9 but this was increased to 4.11 after hydrolysis reaction. However, it remained acidic indicating the acid was not consumed completely. The wastewater became clear after hydrolysis as can be seen from Fig. 8. The disappearance of opacity could not be due to the addition of acid only because wastewater became clear after the hydrolysis reaction and not after the addition of acid; this also can be explained by degradation of phenolic compounds which was found through GC-MS (see Supplementary Information; Fig. S5–S10).

Fig. 9 shows the recorded FTIR spectra for untreated wastewater (*ww*), acetic acid(*aa*), as well as wastewater after 30 min-long hydrolysis of Mg scrap with 12, 18, 24 and 30 wt% aa solution in the wastewater (*ww12aa, ww18aa, ww24aa, ww30aa*, respectively).

In *ww* spectrum the peak located at 3307 cm^{-1}, which was observed in all samples except *aa*, was shifted to the lower wavenumber after hydrolysis and the intensity reduced by increasing *aa* concentration which indicates reduction in OH groups (Dolphen and Thiravetyan, 2011). These results are in agreement with the GC-MS and COD results (Supplementary Information; Figs S5–S10) as the reduction in GC-MS spectra and COD concentration were observed after the hydrolysis.

The absorption due to amide at 1638 cm^{-1} also decreased during hydrolysis, which almost disappeared after hydrolysis reaction and indicates the removal of amide. After hydrolysis, the peak at 1545 cm^{-1} in the spectrum of the brewer's wastewater increases which represents the C=C bond in the aromatic rings of lignin. The characteristic bands at 1415 cm^{-1} can be attributed to the CH_3 asymmetric (asym) deformation which could be observed in the aa sample as well. This shows the presence of aa in the wastewater sample even before the addition of aa and hydrolysis reaction. The disappearance of opacity of the sample (Fig. 8) could be explained by increasing the C–H peak and the reduction in NH_2 or amide peaks (Chandra and Kumar, 2017; Aoyi et al., 2017). The band at 1260 cm^{-1} in the samples after hydrolysis indicates the formation of Si–CH_3 group (Launer, 1987), which is in accordance with the finding through EDS (Fig. 2) and confirms the presence of Si. The appearance of peaks at 1200 cm^{-1} and 1022 cm^{-1} in the samples after hydrolysis reaction may indicate C–H deformation and C–O stretching, respectively, which can be observed in the FTIR spectrum of aa too. A band at 894 cm^{-1} was developed by increasing *aa* concentration which represents the hydrogen-bonded OH- deformation in carboxyl groups (Chandra and Kumar, 2017).

GC-MS analysis of compounds was carried out for all samples including pure aa solution and wastewater without aa before hydrolysis and waste water samples with varied aa content after hydrolysis (Table 2, Figs. S5 to Fig. S10 in Supplementary Information). The main peak of aa was at retention time of 12.443 min. The GC-MS chromatogram of the samples shows several peaks with different areas and intensities, out of which three main peaks of the compounds were detected for wastewater before and after hydrolysis reaction. The first peak with highest area is determined to be Oxime-methoxy-phenyl ($C_8H_9NO_2$) which is a phenolic compound, pollutant A. Phenolic compounds generally can be found in brewery and distillery wastewater, and these compounds are resistant to conventional treatment methods. The quantities of methoxy-phenyl oxime which is a weak oxygen phenolic acid decreased with an increase in the concentration of the aa added. The second peak indicated to be cyclortisiloxane-hexamethyle ($C_6H_{18}O_3Si_3$), pollutant B, which is an organometallic compound. The presence of Si in Mg scrap was confirmed by EDS which consequently led to formation of $C_6H_{18}O_3Si_3$. Hexamethyl cyclotrisiloxane (pollutant B). This is a persistent organic compound which showed an increase in

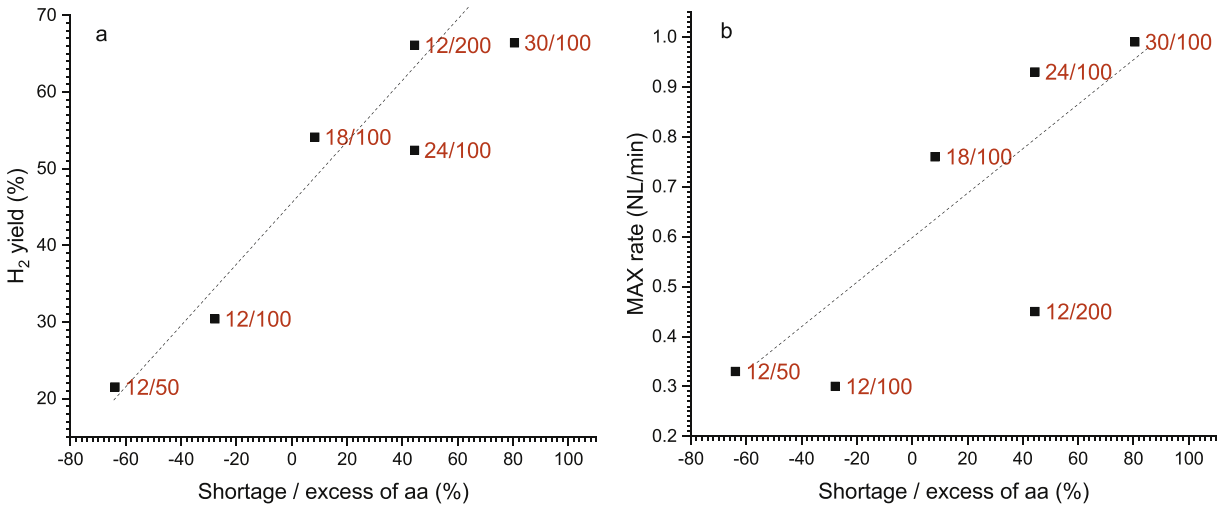

Fig. 7. Dependencies of H_2 yield after 15 min of the hydrolysis (a) and maximum H_2 generation rate (b) during hydrolysis of Mg scrap on the amount of aa in the reaction solution related to stoichiometry of Reaction 2: <0 – shortage, 0 – stoichiometric, >0 – excess. Data labels show aa concentration in wt% (numerator) and volume of the reaction solution in ml (denominator). The dashed trend lines are plotted to guide the eye.

Table 1
Characteristics of *wastewater before and after hydrolysis*.

Characteristic	Wastewater before hydrolysis	Wastewater after addition of aa	Wastewater after hydrolysis
pH	6.17	1.90	4.11
EC (mS)	3.09	1.25	3.57
COD (mg/l)	6130	2356	2304

Experimental conditions: 1-h hydrolysis, 100 ml of wastewater containing 30% aa, at 50 °C, 3.8-g Mg scrap.

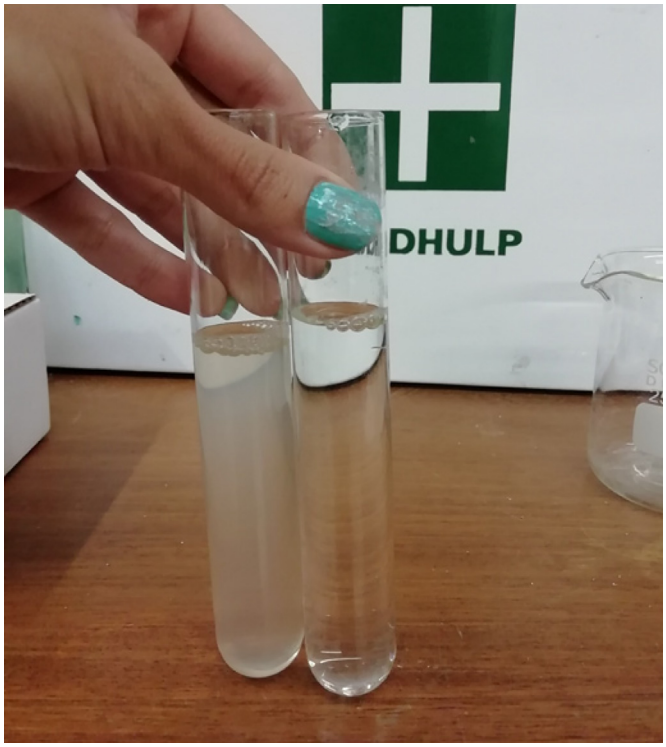

Fig. 8. Photograph of brewery wastewater before addition of aa (left) and after (right) hydrolysis reaction.

concentration with the addition of 12–18%*aa*, however this pollutant reduced significantly (by 62%) with the addition of 30%*aa*. As the amount of aa becomes above 18% (in excess) the amount of

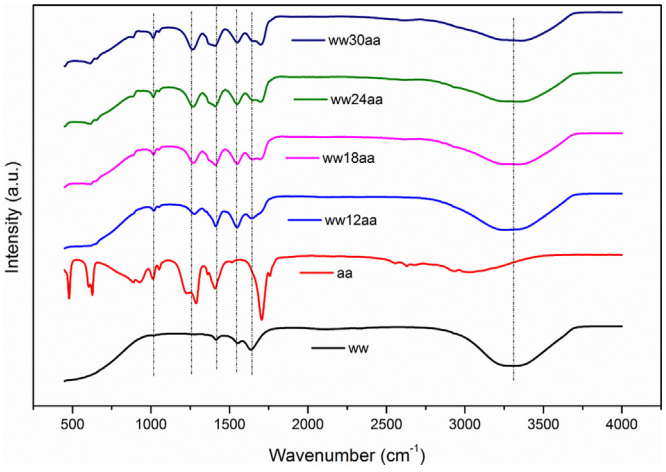

Fig. 9. FTIR spectra of brewer's wastewater (ww), aa (aa), acidified hydrolyzed ww with 12, 18, 24 and 30% aa (ww12aa, ww18aa, ww24aa, ww30aa).

pollutant B decreases significantly. Pollutant C, trimethyl benzaldehyde, which is a phenolic aldehyde is not affected by aa dosages/hydrolysis as the concentration remains almost the same. Other peaks were relatively negligible compared to these three compounds. The changes in the area percentage of Oxime-methoxy-phenyl (Pollutant A), cyclortisiloxane-hexamethyle (Pollutant B) and Trimethyl benzaldehyde (pollutant C) have been shown in Table 2 and Fig. 10. These peaks were not observed in the aa sample.

As can be seen, by increasing the percentage of the *aa*, concentration of pollutants A and B change in the solution. Oxime-methoxy-phenyl (pollutant A) was reduced steadily by increasing

Table 2
GC-MS analysis results for samples before hydrolysis and after hydrolysis with different concentration of aa.

% aa	Sample Name	% Area of pollutant A (Methoxy-phenyl oxime)	%Area of pollutant B (Hexamethyl cyclotrisiloxane)	% Area of pollutant C (Trimethyl benzaldehyde)
0	*ww*	66.11	14.11	3.53
12	*ww12aa*	48.20	20.34	2.94
18	*ww18aa*	46.46	29.97	3.12
24	*ww24aa*	30.49	11.09	3.40
30	*ww30aa*	19.61	5.33	3.40

aa concentration while concentration of cyclortisiloxane-hexamethyle (pollutant B) was increased with the increase of *aa* concentration up to 18% but when increasing to 24% *aa* its concentration reduced, and in 30% *aa* it reduced to the initial concentration. It seems there is a specific optimized amount of aa which produces the best results. Since the wastewater contains different types of organic matters and sometimes the reaction between organic matters and aa could be different at different conditions/concentrations, which sometimes may lead to a reverse reaction. It shows that if the optimum percentage of aa is used in the hydrolysis, it avoids the formation of persistent compounds. There are intermediate products peaks which were observed in samples indicating the degradation of organic compounds in the wastewater during the hydrolysis process in the presence of aa.

The GCMS analysis reveals that the hydrolysis process at the presence of aa was successful for degradation of oximes by 70%. This indicated that the degradation of major toxic phenolic compounds had occurred. It also revealed that at the optimum concentration of 30% aa it does not produce or increase any persistent compound.

Everything taken into account, aa, magnesium ion and its hydrolyzed hydroxyl complexes as well as freshly produced $Mg(OH)_2$ during the hydrolysis contributed to wastewater treatment. The COD could be reduced by reaction of aa with organic compounds present in wastewater and breaking/converting them to the new compounds with lower COD, as could be confirmed by GC-MS results before and after addition of aa (Supplementary Information; Figs S5–S10). Furthermore, $Mg(OH)_2$ is a by-product of hydrogen generation in hydrolysis. It has been reported that freshly produced $Mg(OH)_2$ could act as a coagulant to remove the particles and turbidity of the wastewater (Huang et al., 2012). The magnesium ion and its hydrolyzed hydroxyl complexes could also contribute to coagulation.

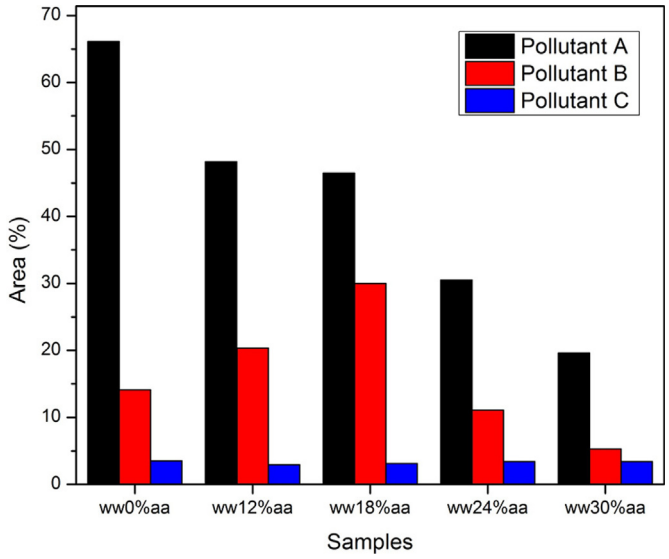

Fig. 10. Changes in the area percentage of Oxime-methoxy-phenyl (pollutant A), cyclortisiloxane-hexamethyle (pollutant B) and Trimethyl benzaldehyde (pollutant C) after hydrolysis reaction at different aa concentrations (0, 12, 18, 24 and 30 wt%aa).

The reduction of amount and concentration of aa used as an accelerator of the hydrolysis reaction is a welcomed development, but this also means the reaction could be incomplete and its kinetics will be sluggish. Furthermore, Mg scrap for hydrogen generation in this study was in compact, not powdered form, and this will further slowdown the reaction kinetics. The results of this study will help to further optimise the hydrolysis process in the future to achieve acceptable reaction yield and kinetics at the minimised amounts of the reaction solution and concentration of aa therein. The reactor configuration could be another factor to be optimized in future study. The optimization and cost analysis are suggested as next steps towards scaling up the process.

4. Conclusions

For the first time, the brewery wastewater solution was used as a source of water for hydrolysis for hydrogen generation using Mg scrap in the presence of acetic acid as an accelerator. The yield of H_2 and the rate of hydrolysis were shown to correlate with the shortage or excess of the acetic acid as compared to stoichiometry of its reaction with $Mg(OH)_2$ formed at the beginning of the process. The control of the stoichiometric ratio was achieved by adjusting the amount of wastewater and concentration of acetic acid. The study reported the highest hydrogen yield (up to 66.4%) within the first 5–15 min of the reaction when the excess of the acetic acid was higher than 44.4%.

When the hydrolysis reaction was incomplete, it resulted in preferable dissolution of Mg while the remaining insoluble deposit contained hydroxides or acetate hydroxides of Al or Al–Mg.

COD of wastewater was reduced by 62% after hydrolysis and consequently there was a reduction of organic matter. Furthermore, FTIR and GC-MS analyses confirmed the degradation of organic compounds simultaneously with hydrolysis process.

On the basis of the results of this study, hydrolysis of Mg scrap using wastewater can be scaled up for utilization in breweries, distilleries and similar industries for treatment of wastewater and onsite hydrogen generation.

CRediT authorship contribution statement

R. Akbarzadeh: Supervision, Conceptualization, Methodology, Investigation, Writing - original draft, Formal analysis, Validation, Writing - review & editing, Project administration. **J.A. Adeniran:** Methodology, Data curation, Formal analysis, Writing - original draft. **M. Lototskyy:** Writing - original draft, Formal analysis, Validation, Writing - review & editing. **A. Asadi:** Writing - original draft, Validation, Writing - review & editing.

Declaration of competing interest

The authors declare that they have no known competing financial interests or personal relationships that could have

appeared to influence the work reported in this paper.

Acknowledgements

Authors appreciate the support of South African Global Excellence Stature (GES) and National Research Foundation (NRF) as well as TIA seed grant support. ML acknowledges the support of Department of Science and Innovation (DSI) of South Africa within Hydrogen South Africa (HySA) National Program (project KP6–S01), as well as NRF (incentive funding grant 109092).

Appendix A. Supplementary data

Supplementary data to this article can be found online at https://doi.org/10.1016/j.jclepro.2020.123198.

References

Adachi-Pagano, M., Forano, C., Besse, J.P., 2003. Synthesis of Al-rich hydrotalcite-like compounds by using the urea hydrolysis reaction control of size and morphology. J. Mater. Chem. 13 (8), 1988–1993. https://doi.org/10.1039/B302747N.

Adeniran, J.A., Akbarzadeh, R., Lototskyy, M., Nyamsi, N.M., Olorundare, O.F., Akinlabi, E.T., et al., 2019. Phase-structural and morphological features, dehydrogenation/re-hydrogenation performance and hydrolysis of nano-composites prepared by ball milling of MgH_2 with germanium. Int. J. Hydrogen Energy 44 (41), 23160–23171. https://doi.org/10.1016/j.ijhydene.2019.06.119.

Akbarzadeh, R., Ghole, V.S., Javadpour, S., 2016. Durable titania films for solar treatment of biomethanated spent wash. Russ. J. Phys. Chem. 90 (10), 2060–2068. https://doi.org/10.1134/S0036024416100228.

Aoyi, O., Onyango, M.S., Apollo, S., Akach, J., Nyembe, N., Otieno, B., et al., 2017. Anaerobic and Photocatalytic Treatment of Textile and Distillery Wastewater in Integrated Fluidized Bed Reactors, pp. 1–201. Pretoria, South Africa. www.wrc.org.za.

Bell, S., Davis, B., Javaid, A., Essadiqi, E., 2006. Final Report on Refining Technologies of Magnesium. Davis Laboratories, Ontario Canada. www.nrcan.gc.ca.

Casey, E.J., Bergeron, R.E., 1953. On the mechanism of the dissolution of magnesium in acidic salt solutions: I. Physical control by surface films. Can. J. Chem. 31, 849–867. https://doi.org/10.1139/v53-115.

Çelik, D., Yıldız, M., 2017. Investigation of hydrogen production methods in accordance with green chemistry principles. Int. J. Hydrogen Energy 42 (36), 23395–23401. https://doi.org/10.1016/j.ijhydene.2017.03.104.

Chandra, R., Kumar, V., 2017. Detection of androgenic-mutagenic compounds and potential autochthonous bacterial communities during in situ bioremediation of post-methanated distillery sludge. Front. Microbiol. 8, 887. https://doi.org/10.3389/fmicb.2017.00887.

Das, S., Mangwani, N., 2010. Recent developments in microbial fuel cells: a review. J. Sci. Ind. Res. 69, 727–731. http://hdl.handle.net/123456789/10294.

Dolphen, R., Thiravetyan, P., 2011. Adsorption of melanoidins by chitin nanofibers. Chem. Eng. J. 166 (3), 890–895. https://doi.org/10.1016/j.cej.2010.11.063.

Engida, T., Mekonnen, A., Wu, J.M., Xu, D., Wu, Z.B., 2020. Review paper on beverage agro-industrial wastewater treatment plant bio-sludge for fertilizer potential in Ethiopa. Appl. Ecol. Environ. Res. 18 (1), 33–57. https://doi.org/10.15666/aeer/1801_033057.

Friedrich, H.E., Mordike, B.L., 2006. Engineering Requirements, Strategies and Examples. Magnesium Technology. Metallurgy, Design Data, Applications, pp. 499–632. https://doi.org/10.1007/3-540-30812-1_8.

Grosjean, M.H., Roué, L., 2006. Hydrolysis of Mg–salt and MgH_2–salt mixtures prepared by ball milling for hydrogen production. J. Alloys Compd. 416 (1–2), 296–302. https://doi.org/10.1016/j.jallcom.2005.09.008.

Hardie, D., Parkins, R.N., 1959. Lattice spacing relationships in magnesium solid solutions. Phil. Mag. 4 (43), 815–825. https://doi.org/10.1080/14786435908238237.

Herrmann, A.P., Janke, H.D., 2001. Cofermentation of rutin and hesperidin during two-stage anaerobic pre-treatment of high-loaded brewery wastewater. Water Res. 35, 2583–2588. https://doi.org/10.1016/S0043-1354(00)00575-3, 11.

Huang, X., Wu, T., Li, Y., Sun, D., Zhang, G., Wang, Y., et al., 2012. Removal of petroleum sulfonate from aqueous solutions using freshly generated magnesium hydroxide. J. Hazard Mater. 219, 82–88. https://doi.org/10.1016/j.jhazmat.2012.03.059.

Kanagachandran, K., Jayaratne, R., 2006. Utilization potential of brewery waste water sludge as an organic fertilizer. J. Inst. Brew. 112, 92–96. https://doi.org/10.1002/j.2050-0416.2006.tb00236.x, 2.

Kannabiran, B., Pragasam, A., 1993. Effect of distillery effluent on seed germination, seedling growth and pigment content of Vigna mungo (L.) Hepper (CVT 9). Geobios (Jodhpur) 20, 108-108.

Kushch, S.D., Kuyunko, N.S., Nazarov, R.S., 2011. Hydrogen-generating compositions based on magnesium. Int. J. Hydrogen Energy 36 (1), 1321–1325. https://doi.org/10.1016/j.ijhydene.2010.06.115.

Launer, P.J., 1987. Infrared analysis of organosilicon compounds: spectra-structure correlations. In: Silicone Compounds Register and Review, vol. 100. https://www.researchgate.net/publication/272481071.

Maintinguer, S.I., Lazaro, C.Z., Pachiega, R., Varesche, M.B.A., Sequinel, R., de Oliveira, J.E., 2017. Hydrogen bioproduction with Enterobacter sp. isolated from brewery wastewater. Int. J. Hydrogen Energy 42 (1), 152–160. https://doi.org/10.1016/j.ijhydene.2016.11.104.

Matković, V.L., Manojlović, V.D., Sokić, M.D., Marković, B.R., Gulišija, Z.P., Žj, Kamberović, 2014. Optimal conditions of vacuum distillation process for obtaining the high grade pure magnesium. Tehnika 69 (1), 58–62. https://10.5937/tehnika1401058M.

Mielcarek, A., Janczukowicz, W., Ostrowska, K., Jóźwiak, T., Kłodowska, I., Rodziewicz, J., Zieliński, M., 2013. Biodegradability evaluation of wastewaters from malt and beer production. J. Inst. Brew. 119, 242–250. https://doi.org/10.1002/jib.92.

Mohanakrishna, G., Mohan, S.V., Sarma, P.N., 2010. Bio-electrochemical treatment of distillery wastewater in microbial fuel cell facilitating decolorization and desalination along with power generation. J. Hazard Mater. 177 (1–3), 487–494. https://doi.org/10.1016/j.jhazmat.2009.12.059.

Ni, M., Leung, D.Y., Leung, M.K., Sumathy, K., 2006. An overview of hydrogen production from biomass. Fuel Process. Technol. 87 (5), 461–472. https://doi.org/10.1016/j.fuproc.2005.11.003.

Pandey, J., Agrawal, M., 1994. Evaluation of air pollution phytotoxicity in a seasonally dry tropical urban environment using three woody perennials. New Phytol. 126 (1), 53–61. https://doi.org/10.1111/j.1469-8137.1994.tb07529.x.

Pant, D., Adholeya, A., 2007. Biological approaches for treatment of distillery wastewater: a review. Bioresour. Technol. 98 (12), 2321–2334. https://doi.org/10.1016/j.biortech.2006.09.027.

Patwardhan, A.D., 2017. Industrial Wastewater Treatment. PHI Learning Pvt. Ltd.

Radha, A.V., Kamath, P.V., Shivakumara, C., 2007. Order and disorder among the layered double hydroxides: combined Rietveld and DIFFaX approach. Acta Crystallogr. Sect. B Struct. Sci. 63 (2), 243–250. https://doi.org/10.1107/S010876810700122X.

Rothabauer, R., Zigan, F., O'Daniel, H., Verfeinerung, D.S.D.B., 1967. Al[OH]3 Einschliesslich eines Vorschlags für die H-Positionen. Z. Kristallogr. 125, 317–331.

Saccone, A., Cacciamani, G., De Negri, S., Ferro, R., 2002. The Al-Er-Mg ternary system Part I: experimental investigation. J. Phase Equil. 23 (1) https://doi.org/10.1361/105497102770332180, 29-27.

Shah, M.P., Rodriguez-Couto, S. (Eds.), 2019. Microbial Wastewater Treatment. Elsevier.

Sharmila, V.G., Banu, J.R., Kim, S.H., Kumar, G., 2020. A review on evaluation of applied pretreatment methods of wastewater towards sustainable H2 generation: energy efficiency analysis. Int. J. Hydrogen Energy. https://doi.org/10.1016/j.ijhydene.2020.01.081.

Simate, G.S., Cluett, J., Iyuke, S.E., Musapatika, E.T., Ndlovu, S., Walubita, L.F., Alvarez, A.E., 2011. The treatment of brewery wastewater for reuse: state of the art. Desalination 273 (2–3), 235–247. https://doi.org/10.1016/j.desal.2011.02.035.

Sui, R., Lo, J.M.H., Lavery, C.B., Deering, C.E., Wynnyk, K.G., Chou, N., et al., 2018. Sol–gel-derived 2D nanostructures of aluminum hydroxide acetate: toward the understanding of nanostructure formation. J. Phys. Chem. C 122 (9), 5141–5150. https://doi.org/10.1021/acs.jpcc.7b12490.

Uan, J.Y., Cho, C.Y., Liu, K.T., 2007. Generation of hydrogen from magnesium alloy scraps catalyzed by platinum-coated titanium net in NaCl aqueous solution. Int. J. Hydrogen Energy 32 (13), 2337–2343. https://doi.org/10.1016/j.ijhydene.2007.03.014.

Uan, J.Y., Yu, S.H., Lin, M.C., Chen, L.F., Lin, H.I., 2009. Evolution of hydrogen from magnesium alloy scraps in citric acid-added seawater without catalyst. Int. J. Hydrogen Energy 34 (15), 6137–6142. https://doi.org/10.1016/j.ijhydene.2009.05.133.

Uesugi, H., Sugiyama, T., Nakatsugawa, I., 2010. Production of Hydrogen Storage Material MgH2 and its Applications. Blocoke Lab. Ltd, Japan. https://pdfs.semanticscholar.org/.

Von Batchelder, F.W., Raeuchle, R.F., 1957. Lattice constants and Brillouin Zone overlap in dilute magnesium alloys. Phys. Rev. 105 (1), 59. https://doi.org/10.1103/PhysRev.105.59.

Werkneh, A.A., Beyene, H.D., Osunkunle, A.A., 2019. Recent advances in brewery wastewater treatment; approaches for water reuse and energy recovery: a review. Environ. Sustain. 1–11. https://doi.org/10.1007/s42398-019-00056-2.

Xavier, C., Kiyohara, P.K., Souza Santos, H., Souza Santos, P., 1998. Preparation of crystalline aluminium hydroxiformate and acetate using aluminium powder. An Acad. Bras Ciências 70 (3), 411–422. https://repositorio.usp.br/item/000992645.